



HAL
open science

The Q-loop Disengages from the First Intracellular Loop during the Catalytic Cycle of the Multidrug ABC Transporter BmrA

Olivier Dalmas, Cedric Orelle, Anne-Emmanuelle Foucher, Christophe Geourjon, Serge Crouzy, Attilio Di Pietro, Jean-Michel Jault

► **To cite this version:**

Olivier Dalmas, Cedric Orelle, Anne-Emmanuelle Foucher, Christophe Geourjon, Serge Crouzy, et al.. The Q-loop Disengages from the First Intracellular Loop during the Catalytic Cycle of the Multidrug ABC Transporter BmrA. *Journal of Biological Chemistry*, 2005, 280 (44), pp.36857-36864. 10.1074/jbc.m503266200 . hal-01988190

HAL Id: hal-01988190

<https://hal.science/hal-01988190>

Submitted on 28 Jan 2019

HAL is a multi-disciplinary open access archive for the deposit and dissemination of scientific research documents, whether they are published or not. The documents may come from teaching and research institutions in France or abroad, or from public or private research centers.

L'archive ouverte pluridisciplinaire **HAL**, est destinée au dépôt et à la diffusion de documents scientifiques de niveau recherche, publiés ou non, émanant des établissements d'enseignement et de recherche français ou étrangers, des laboratoires publics ou privés.

The Q-loop Disengages from the First Intracellular Loop during the Catalytic Cycle of the Multidrug ABC Transporter BmrA*

Received for publication, March 24, 2005, and in revised form, July 29, 2005 Published, JBC Papers in Press, August 17, 2005 DOI 10.1074/jbc.M503266200

Olivier Dalmas^{‡1}, Cédric Orelle^{‡1}, Anne-Emmanuelle Foucher[§], Christophe Geourjon[‡], Serge Cruzy[§], Attilio Di Pietro[‡], and Jean-Michel Jault^{§2}

From the [‡]Institut de Biologie et Chimie des Protéines, Unité Mixte de Recherche 5086 CNRS-UCBL1 and IFR 128, 7 Passage du Vercors, 69367 Lyon Cedex 07, France and [§]Laboratoire de Biophysique Moléculaire et Cellulaire, DRDC, Unité Mixte de Recherche 5090 CNRS/Commissariat à l'Énergie Atomique/UJF, Commissariat à l'Énergie Atomique 17 Rue des Martyrs, Bâtiment K, 38054 Grenoble Cedex 9, France

The ATP-binding cassette is the most abundant family of transporters including many medically relevant members and gathers both importers and exporters involved in the transport of a wide variety of substrates. Although three high resolution three-dimensional structures have been obtained for a prototypic exporter, MsbA, two have been subjected to much criticism. Here, conformational changes of BmrA, a multidrug bacterial transporter structurally related to MsbA, have been studied. A three-dimensional model of BmrA, based on the "open" conformation of *Escherichia coli* MsbA, was probed by simultaneously introducing two cysteine residues, one in the first intracellular loop of the transmembrane domain and the other in the Q-loop of the nucleotide-binding domain (NBD). Intramolecular disulfide bonds could be created in the absence of any effectors, which prevented both drug transport and ATPase activity. Interestingly, addition of ATP/Mg plus vanadate strongly prevented this bond formation in a cysteine double mutant, whereas ATP/Mg alone was sufficient when the ATPase-inactive E504Q mutation was also introduced, in agreement with additional BmrA models where the ATP-binding sites are positioned at the NBD/NBD interface. Furthermore, cross-linking between the two cysteine residues could still be achieved in the presence of ATP/Mg plus vanadate when homobifunctional cross-linkers separated by more than 13 Å were added. Altogether, these results give support to the existence, in the resting state, of a monomeric conformation of BmrA similar to that found within the open MsbA dimer and show that a large motion is required between intracellular loop 1 and the nucleotide-binding domain for the proper functioning of a multidrug ATP-binding cassette transporter.

ATP-binding cassette (ABC)³ transporters form one of the largest protein families in all species and are involved in the cellular or subcel-

lular uptake or export of an extraordinary variety of substrates, including ions, sugars, lipids, amino acids, organic compounds, peptides, or even proteins (1). Several human ABC transporters are associated with genetic diseases such as cystic fibrosis and adrenoleucodystrophy, whereas others are responsible for multidrug resistance (MDR) phenotype of cancer cells, namely P-glycoprotein, MRP1, and BCRP (2, 3). In microorganisms as well, many medically relevant members are found, including MDR efflux pumps such as pMDR1 in parasites, Pdr5p in yeast, and LmrA in bacteria (4). The core structure of ABC transporters is composed of four domains: two transmembrane domains (TMDs), quite divergent in sequence and topology, are involved in substrate translocation, and two nucleotide-binding domains (NBDs) energize the transporters through ATP binding and hydrolysis (5). These four domains are either found on the same polypeptide (full-length transporter) or on separate subunits, from two (half-transporter) to four (1). The NBDs are highly conserved in sequence and show a similar fold regardless of their origin and function (prokaryotic *versus* eukaryotic and importers *versus* exporters), suggesting that all ABC transporters share a similar overall mechanism for energy transduction (6). Four high resolution three-dimensional structures of complete ABC transporters are available: the lipid A exporter, MsbA, was crystallized either as an open (EcMsbA) or a closed (VcMsbA and StMsbA) dimer, and the vitamin B12 importer, BtuCD, shows a closed compact structure (7–10). Although the NBD structure in BtuCD agreed well with the tertiary structure of isolated NBDs, the one found in VcMsbA was only partly in agreement with other known structures, showing an unprecedented fold. This new fold was therefore regarded as a possible consequence of crystal packing constraints (6, 11). An even stronger skepticism greeted the EcMsbA structure because the partially resolved NBDs are oriented toward the outside of the dimer interface with an unusually limited TMD interface (6, 11–14). Thus, a complete rotation of the NBDs with respect to the TMDs would be required during the catalytic cycle to reconstitute the two ATP-binding sites at the NBDs interface in a conformation supported by many pieces of biochemical and structural evidence (15–19). The third MsbA structure very recently obtained, StMsbA, appears more consensual than the two previous ones and might reflect a post-hydrolytic conformational state (10).

We have previously shown that the sequence of BmrA (Bacillus multidrug resistance ATP), a new multidrug resistance bacterial half-ABC transporter (20), was akin to that of MsbA; on the other hand, EcMsbA was found to exhibit some drug efflux abilities (21). Here, several three-dimensional models of BmrA were built, using EcMsbA, VcMsbA, or StMsbA structure as template. In contrast to the different three models based on the closed conformation of MsbA (two based solely either on

* This work was supported by CNRS Grant PGP 2002 (to A. D. P.), a CNRS Young Investigator ATIP Program grant (to J.-M. J.), and ACI IMPBio Grant IMPB027 from the Ministère de la Recherche (to A. D. P. and J.-M. J.). The costs of publication of this article were defrayed in part by the payment of page charges. This article must therefore be hereby marked "advertisement" in accordance with 18 U.S.C. Section 1734 solely to indicate this fact.

¹ Recipients of fellowships from both the Ministère de la Recherche and Fondation pour la Recherche Médicale.

² To whom correspondence should be addressed. Tel.: 33-4-38-78-31-19; Fax: 33-4-38-78-54-87; E-mail: jean-michel.jault@cea.fr.

³ The abbreviations used are: ABC, ATP-binding cassette; BmrA, Bacillus multidrug resistance ATP; EcMsbA, *E. coli* MsbA; ICL1, intracellular loop 1; NBD, nucleotide-binding domain; StMsbA, *S. typhimurium* MsbA; TMD, transmembrane domain; VcMsbA, *V. cholerae* MsbA; DTT, dithiothreitol; PDB, Protein Data Bank.

Conformational Changes in a Multidrug ABC Transporter

StMsbA or VcMsbA, plus two chimeric ones based on VcMsbA for the TMD and either BtuD or MJ0796 for the dimeric association of the NBDs), the model based on the open conformation of EcMsbA suggested a close proximity between residues of the first intracellular loop, ICL1 (also known as ICD1 (7)), that belongs to the TMDs and residues of the so-called Q-loop of NBDs. Introducing two cysteine residues simultaneously in these sequences allowed the formation of disulfide bonds, resulting in an inactive transporter for both drug efflux and ATPase activity, whereas addition of DTT restored both activities. Furthermore, addition of ATP/Mg plus vanadate prevented the disulfide bond formation in a BmrA double mutant, whereas ATP/Mg alone was sufficient when the additional E504Q mutation that abolishes ATP hydrolysis was simultaneously introduced. In the vanadate-trapped state, the cysteine residues introduced in wild-type BmrA could still be cross-linked upon addition of homobifunctional reagents of sufficient lengths. Our results clearly show that during the catalytic cycle of BmrA the NBDs must move away from the TMDs, thereby preventing the disulfide bond formation; this conformational motion between the two domains is likely to play a key role in the catalytic cycle of ABC multidrug transporters.

EXPERIMENTAL PROCEDURES

Unless otherwise stated, all chemicals and restriction enzymes were purchased from Sigma and Promega, respectively.

Site-directed Mutagenesis—pET23b(+)/C436S was used as a template for site-directed mutagenesis to introduce a single cysteine using Kunkel's method as previously described (22). To screen for positive clones, oligonucleotides with the following sequences were designed to introduce the desired mutations and to simultaneously introduce or remove a restriction site without modifying the protein sequence: N118C, ACGGCTGACTGTTTTCTCCTGAAGCACATGTATCGAAATAA, A119C, GACTGTTTTCTCCTGAACAATTTGTATCGAAAT, and T123C, CGTTACACGGCTGACACATTCTCCTGAAGCATTGTAT removing an AccIII restriction site; V124C ATCGTTCGTTACACGGCTGCAGGTTTCTCCGGAAGCA adding a PstI restriction site; V127C ACCATCGTATCGTTTTGTACAACGGCTGACTGTT adding a BsrGI (New England Biolabs) restriction site; S424C, TGTC-CCGGACATTAATGGGCATTCTGTGATACA adding an AsnI restriction site; M427C TTTTCTCTGATTGTTCCGGAACATAACGGGCTTTC adding an AccIII restriction site; S428C, ATATTTTCTCTGATGGTACCGCACATTAACGGGC adding a KpnI restriction site. E504Q was constructed as previously described (22). All mutations were verified by DNA sequencing. Double cysteine mutants were constructed by a subcloning technique. Basically, 5 μ g of pure pET23b(+)/C436S containing a single cysteine codon were digested by 5 units of NheI and StuI. Fragments were purified by 0.7% agarose gel electrophoresis. After ligation, positive clones were selected by digestion pattern. BmrA T123C-S428C-E504Q was made using the same subcloning technique with SacII and BspI (New England Biolabs) restriction enzymes.

Preparation of BmrA-enriched Membranes—*E. coli* BmrA-enriched membranes were prepared as described (23) and kept frozen in liquid nitrogen. Protein concentration of membranes was estimated by a Lowry protein assay (Pierce) after precipitation of proteins by trichloroacetic acid. Typically, protein concentrations were in the range of 50 to 70 mg/ml.

ATPase Assay—ATPase activity was monitored using a P_i release method as previously described (24). Briefly, 1–4 μ l of 10-fold diluted membranes were incubated in a 50-mM Hepes, pH 8.0, buffer contain-

ing 50 mM NaCl, 5 mM $MgCl_2$, 5 mM ATP, 0.5 mM EGTA, 10 mM NaF, 10 mM NaN_3 , and 1 mM ouabain.

Hoechst Transport—Time course fluorescence intensity was monitored on a Photon Technology International Quanta Master I fluorimeter, using excitation and emission wavelengths of 355 and 457 nm and slit widths of 2 and 4 nm as previously described (23). Membrane vesicles were treated by either 200 μ M $CuSO_4$ or 5 mM DTT for 30 min at 30 °C. Membranes were washed twice by ultracentrifugation at 100,000 \times g for 1 h. Then, 500 μ g of total protein were added into a 3-ml cuvette containing 2 ml of 50 mM Hepes/KOH, pH 8.0, 2 mM $MgCl_2$, 50 mM NaCl, 40 μ g of pyruvate kinase (E.C.2.7.1.40), and 4 mM phosphoenolpyruvate. After ~1 min of incubation at 37 °C, 2 μ M Hoechst 33342 (2'-[4-ethoxyphenyl]-5-[4-methyl-1-piperazinyl]-2,5'-bis-1H-benzimidazole) was added, and the fluorescence was recorded for 1–2 min. ATP was then added to a final concentration of 2 mM, and the fluorescence intensity was further monitored for several minutes.

Cross-linking Analysis—*E. coli* membrane vesicles containing overexpressed BmrA were diluted at 5 μ g/ μ l (final volume of 50 μ l) in a buffer containing 50 mM Hepes, pH 7.0, 50 mM NaCl, 5 mM $MgCl_2$. When indicated, membrane vesicles were incubated in the presence of effectors for 20 min at room temperature. Cysteine oxidation was promoted by addition of 200 μ M $CuSO_4$, and samples were incubated for either 1 h on ice or 30 min at 30 °C. For the different methanethiosulfonate cross-linkers (Toronto Research Chemicals, Toronto, Canada), membrane vesicles were incubated on ice for 5 min with 200 μ M methanethiosulfonate compound. When indicated, free sulfhydryl groups were modified by addition of 10 mM *N*-ethylmaleimide for 30 min at 25 °C. 15 μ g of protein were resolved by SDS-PAGE (10%) using a Laemmli buffer in the absence of reducing reagent and stained with Coomassie Blue R250.

Molecular Modeling—The three-dimensional model of BmrA based on EcMsbA was built by using Geno3D, a comparative molecular modeling program for proteins (25). Protein structures of TAP1 (PDB accession code 1JJ7-A; the closest homologue whose structure found in the PDB has been published) and EcMsbA (PDB accession code 1JSQ-A) were taken as templates for molecular modeling of the open monomeric conformation of BmrA. On the basis of sequence identity after sequence alignment with BmrA, distance restraints and dihedral angles were calculated on the template structures. These measurements were performed for all common atoms revealed by alignment of BmrA with the templates. The approach used in Geno3D allows reconstruction of the protein three-dimensional model by fragments. For that, it is necessary that sequence alignment between query protein and templates show partial overlapping sequences. In these segments, the generated restraints resulted from both templates simultaneously. The CNS 1.1 program (26) was used to generate the model by a distance geometry approach similar to that used in modeling from NMR experiments. Each structure was regularized by simulated annealing (2000 steps) and energy minimization (2000 steps). Ten models were built, all exhibiting closely similar features, and were superimposed with the ANTHEPROT three-dimensional package by minimizing the root mean square deviation between α carbons (27). Mirror images were eliminated on the basis of energy calculation. The model retained was that with the lowest energy (–19334 kcal/mol) and regular chemical features, and its quality was assessed with the PROCHECK tools (28) (91% of residues are located in the favorable region of the Ramachandran plot). The visualization of the molecule was performed using Pymol software (Delano Scientific LLC).

Two “closed” BmrA models based solely on the VcMsbA template (PDB accession code 1PF4) were built using either the same program as

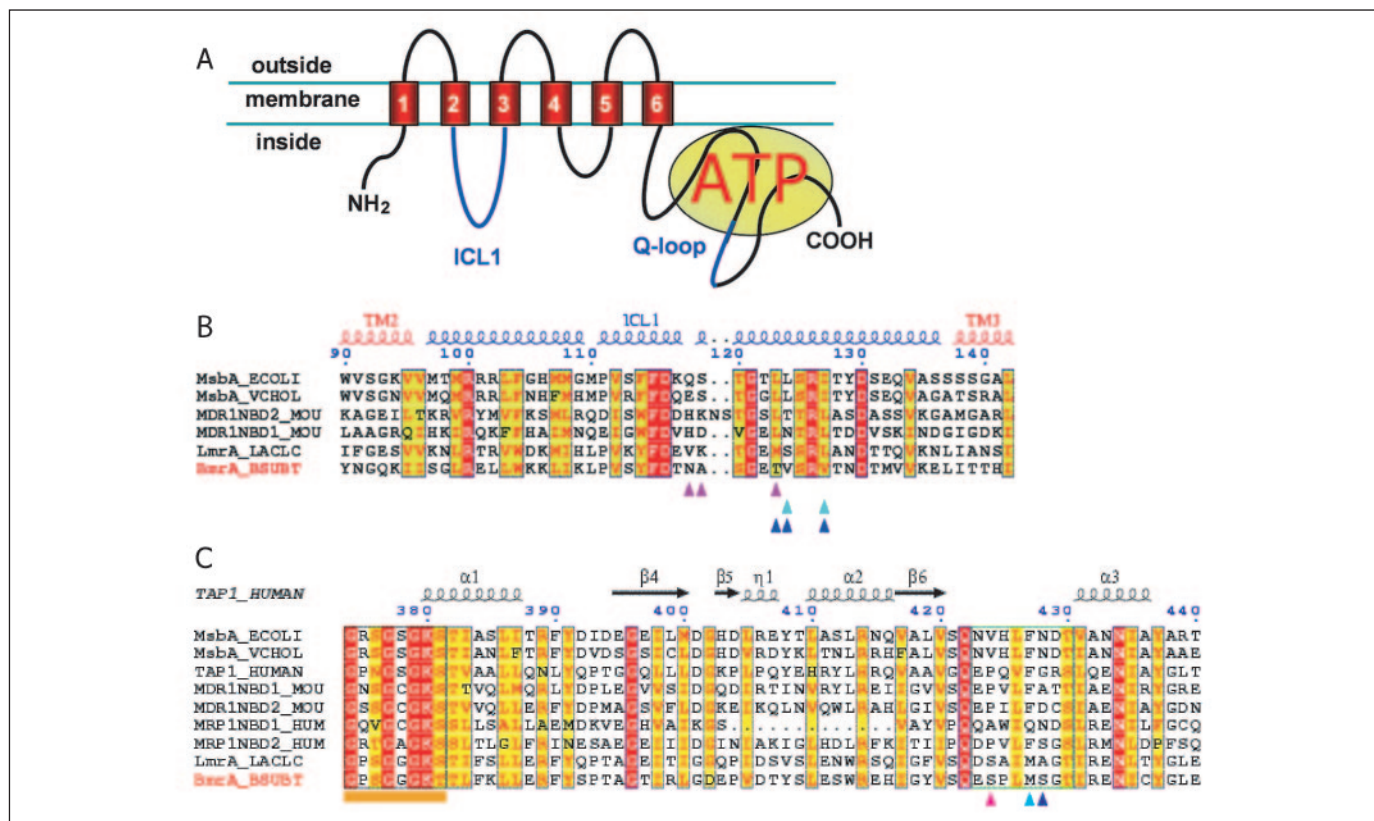


FIGURE 1. Topology of BmrA and sequence alignments. *A*, predicted topology of BmrA and location of the first intracellular loop (ICL1) and the Q-loop within the NBD. The transmembrane helices are depicted by rectangular red boxes, numbered 1–6; the ATP-binding site is schematized by a yellow oval. *B* and *C*, sequence alignments in ABC transporters around ICL1 and the Q-loop, respectively. Sequences were obtained on the ExPASy server (us.expasy.org/), and the alignment was generated by Clustal W (1.8) on the NPS@ server (npsa-pbil.ibcp.fr). These two panels were made with ESPrnt 2.0 (prodes.toulouse.inra.fr/ESPrnt/). *ECOLI*, *E. coli*; *VCHOL*, *V. cholerae*; *LACL*, *L. lactis*; *BSUBT*, *B. subtilis*; *MOU*, mouse; *HUM*, human; *TM2* and *TM3*, transmembrane helices 2 and 3. The numbering used corresponds to the BmrA sequence. Blue frames were drawn when at least 50% of the residues were identical (white characters in red boxes for fully conserved residues, red characters in yellow boxes otherwise). Secondary structures and boundaries of TM2, TM3, and ICL1 were taken from Ref. 7. The position of Walker A is underlined in orange and that of the Q-loop is boxed in green. The BmrA residues mutated are indicated by pink, cyan, and blue arrowheads according to the different double mutants created. The secondary structure of TAP1 is shown above the sequences.

for the open BmrA model or, alternatively, the MODELLER program (version 7v7) (29), which allows building models faster than the previous method. Both models gave essentially similar parameters when assessing their quality, and similar distance values were obtained between the two residues replaced by cysteines (only the values obtained from the model made by the MODELLER program are shown in TABLE ONE). Another closed BmrA model was built with the same program based on homology with the recently resolved structure of MsbA from *Salmonella typhimurium* (PDB accession code 1Z2R). The missing residues in the structures of VcMsbA and StMsbA have been left out in the models of BmrA. Ten models were generated with the MODELLER program from both VcMsbA and StMsbA, and the models with the lowest objective functions were kept. They will hereafter be referred to as ModVc and ModSt.

To build the closed BmrA models with an NBD/NBD interface based on either BtuCD (VcMsbA/BtuCD) or MJ0796 (VcMsbA/MJ0796) NBDs dimers, the NBD of BmrA was first modeled using the NBD of TAP1 as a template. The sequences of BmrA (from Glu-324) and TAP1 were aligned with CLUSTALW (alignment score 532) on the NPS@ web server (npsa-pbil.ibcp.fr), and again 10 models were generated with MODELLER from this alignment. The model with the lowest objective function (1431.7) was retained. Then the NBD model of BmrA was fitted sequentially to each of the two NBDs of the vitamin B12 transporter BtuCD (PDB accession code 1L7V) and of the archaeal ABC transporter MJ0796 (PDB accession code 1L2T), both being crystallized in a closed conformation with a correct positioning of the NBD/NBD

interface. The difference between the two structures lies in the fact that BtuCD was crystallized in the absence of ATP (replaced by cyclo-tetranadate) in a “nonenergized” state, whereas the NBDs from MJ0796 were obtained in the presence of ATP/Na⁺. The fit was done by least square superposition of the four β strands corresponding to the conserved core β sheet of the NBDs, namely residues Val-369 to Val-373, Ile-417 to Val-420, Ile-498 to Leu-501, and Thr-529 to Ile-533 in BmrA. Backbone atoms only were selected for the fits resulting in root mean square deviations of 1.84 and 1.81 Å for the fit to BtuCD and MJ0796, respectively. (Similar root mean squares were obtained for the fits of the two NBDs.) In the next step, the two NBDs now forming a correct interface were docked as a rigid body onto the TMDs built by homology from *Vibrio cholerae* (ModVc). This was done by least square superposition of the three β strands comprising residues Gly-418 to Ser-421, Ile-498 to Leu-501, and Thr-529 to Ile-533 in BmrA, with final root mean square deviations of 3.9 and 3.7 Å for the anchoring of the NBDs based on BtuCD (ModBtu) and on MJ0796 (ModMJ), respectively. Finally, the four models of complete BmrA dimers in the closed state, including residues Lys-9 to Glu-562 (the loop Phe-202 to Leu-236 was excluded), ModVc, ModSt, ModBtu, and ModMJ were relaxed by energy minimization with the Molecular Dynamics program CHARMM (30). Strong harmonic restraints (force constant 5 kcal/mol/Å²) were applied on the backbone atoms of the models during the minimization to prevent unfolding or large atomic displacements that might be caused by the absence of solvent and lipids in this simple molecular modeling. Total (Etot.) and harmonic (Eharm.) restraint

Conformational Changes in a Multidrug ABC Transporter

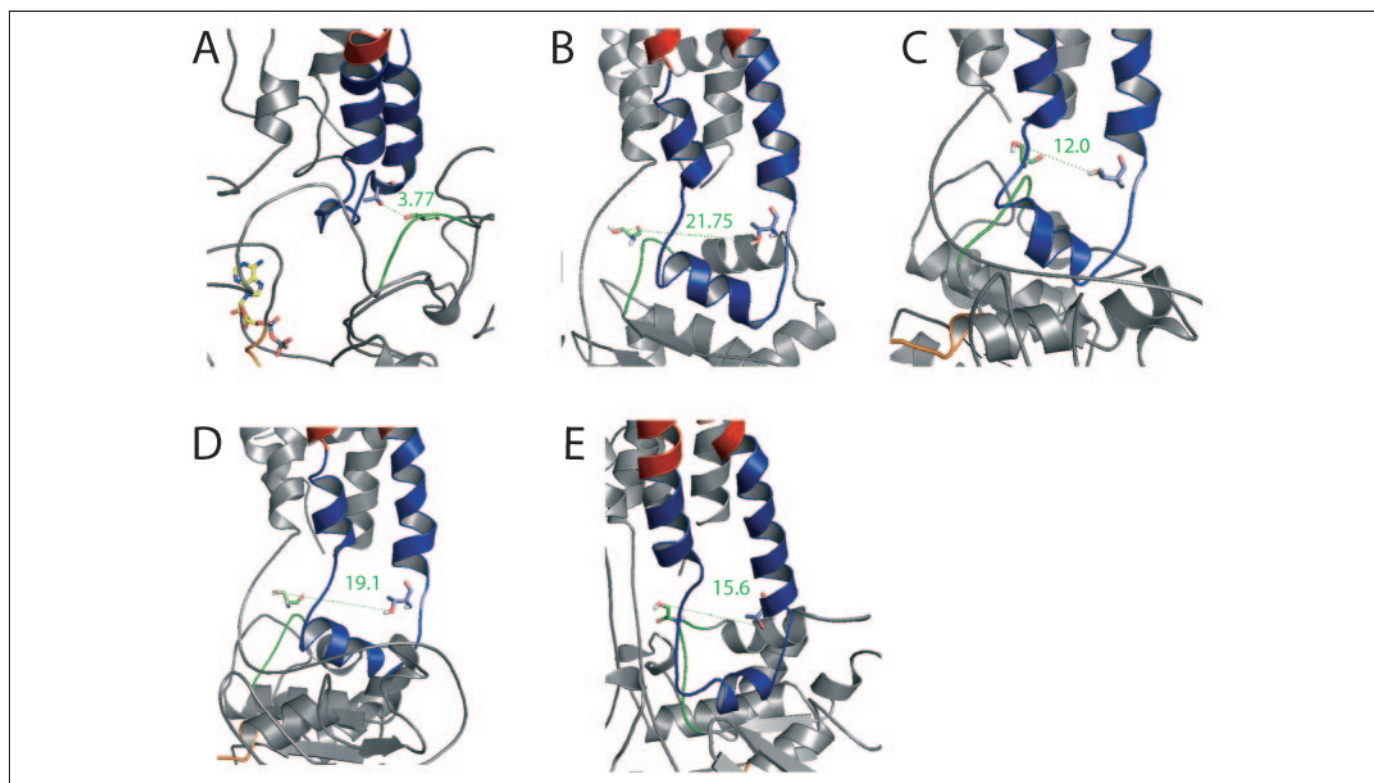


FIGURE 2. Different three-dimensional models of BmrA. A, close-up view of the three-dimensional model of BmrA based on both the EcMsba template and on the TAP1 structure for the missing part of the NBD. The NBD is shown in *gray* and ICD1 in *blue*. The same color coding as in Fig. 1, B and C, was used to identify the different parts of BmrA. The ADP coordinates were taken from the TAP1 structure and drawn as a *stick model* colored by elements. The putative distance between Thr-123 in the ICD1 and Ser-428 in the NBD is shown. B–E represent the same close-up view of the inter-residue distance using different BmrA models with the same code color as in panel A. Panel B was taken from the three-dimensional BmrA model based solely on VcMsba template. Panels C and D were taken from two different chimeric three-dimensional models, both based on VcMsba template for the TMD and on either BtuD or MJ0796 template for the NBD. Panel E was taken from the three-dimensional BmrA model based solely on StMsba template. This figure was drawn using PyMol (Delano Scientific LLC; www.pymol.org).

TABLE ONE

Distances between two residues simultaneously replaced by a cysteine, according to the different models

Distances were obtained from the different BmrA models built as described under “Experimental Procedures.” (+) or (–) indicates that disulfide bond was detected, or not, after a prior incubation with cupric ion (see Fig. 2). (+++) indicates that disulfide bond was formed even in the absence of cupric ion.

Residues	S-S bond formation	Distances between the residues					
		Å					
		Open BmrA (EcMsba)	Closed BmrA (VcMSBA)	Closed BmrA (VcMsba/BtuD)	Closed BmrA (VcMsba/MJ0796)	Closed BmrA (StMsba)	
Ser-424	Asn-118	+	3.5	18.4	11.6	13.8	9.1
	Ala-119	+	4.9	22.1	17.3	18.7	13.7
	Thr-123	–	7.1	28.7	18.0	20.9	15.3
Met-427	Val-124	–	8.2	22.6	13.8	20.3	18.1
	Val-127	–	4.1	17.8	11.3	17.6	14.9
Ser-428	Thr-123	+++	3.8	21.75	12.0	19.1	15.6
	Val-124	+	4.2	28.3	18.0	25.4	20.7
	Val-127	–	9	24.0	13.7	21.9	15.0

energies were as follows: ModVc, $E_{tot} = -25280$ and $E_{harm} = 216$; ModSt, $E_{tot} = -25950$ and $E_{harm} = 164$; ModBtu, $E_{tot} = -21481$ and $E_{harm} = 1188$; and ModMJ, $E_{tot} = -25283$ and $E_{harm} = 818$. The model built from BtuCD appears to be the least stable and shows the largest restraint energy term, whereas the model made from *S. typhimurium* is the most stable. Interestingly, the chimeric model built from Vc/Msba and MJ0796 is more stable by 600 kcal/mol (if we subtract the restraint term) than the model made by direct homology from VcMsba alone. PROCHECK results show that all models have more than 95% of amino acids in the allowed Ramachandran regions

(96.5, 96.7, 95.9, and 96.7% for ModVc, ModSt, ModBtu, and ModMJ, respectively).

RESULTS

The fairly good homology found between BmrA and Msba (20) allowed us to build BmrA models based on either the open or the closed conformation of Msba. In the open BmrA model, the first intracellular loop of TMD was found very close to the Q-loop of NBD (Figs. 1A and 2A). To experimentally test this model, double mutants were created where two cysteine residues were simultaneously introduced into a fully

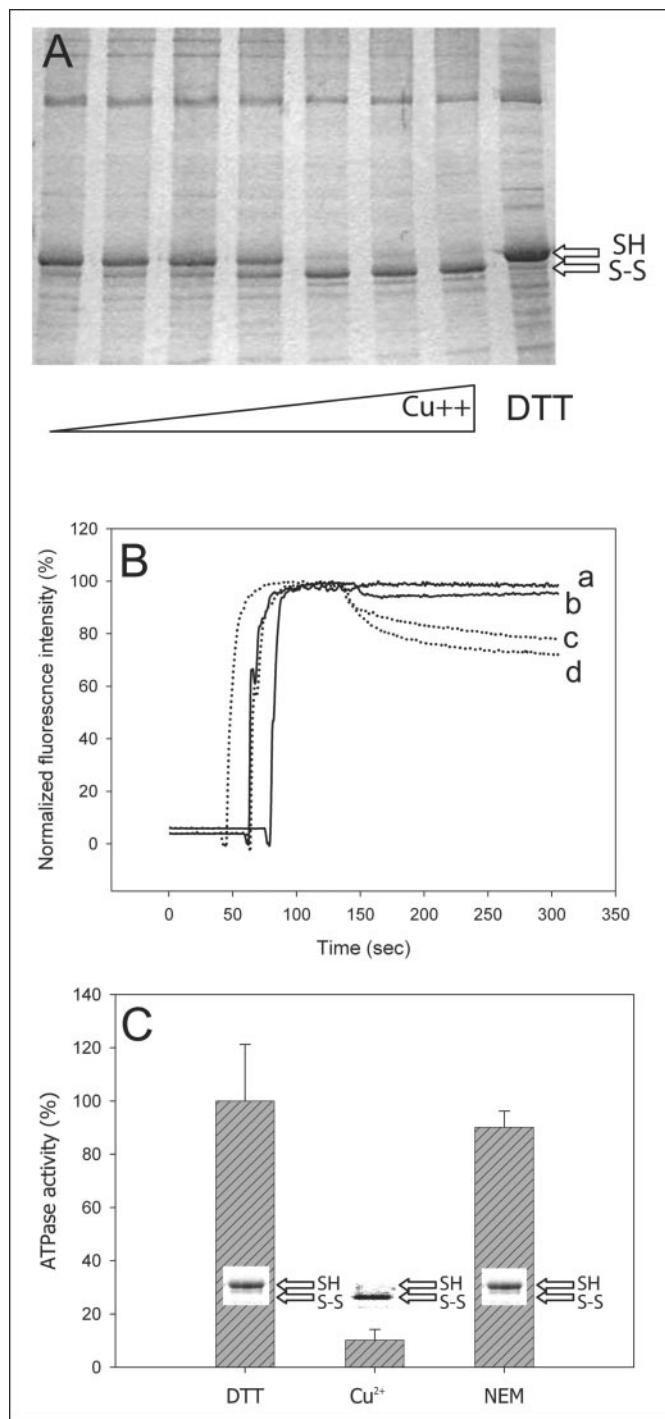


FIGURE 3. The flexibility between NBD and ICL1 is essential to BmrA function. *A*, *E. coli* membrane vesicles containing the overexpressed double mutant of BmrA (S428C/T123C) were incubated in a degassed buffer with increasing concentration of CuSO_4 (0–2 mM), and 15 μg of total protein was analyzed by non-reducing SDS-PAGE. The right lane corresponds to a sample incubated with 2 mM CuSO_4 and then treated with 5 mM DTT for 30 min. *B*, the formation of disulfide bonds inhibits the transport activity of BmrA. The S424C/A119C (*a* and *c*) or S428C/T123C (*b* and *d*) double mutants were incubated with 200 μM CuSO_4 (*a–d*) for 30 min, and transport activities of Hoechst were either measured directly (*a* and *b*) or after a subsequent incubation with 5 mM DTT for 30 min (*c* and *d*). *C*, *E. coli* membrane vesicles containing the overexpressed S428C/T123C double mutant were assayed (in triplicate) for ATPase activity after treatment with either 5 mM DTT, 200 μM CuSO_4 , or 10 mM *N*-ethylmaleimide (NEM) for 30 min at 25 °C. A sample of 15 μg of total protein was withdrawn from the incubation samples and analyzed by SDS-PAGE without reducing agent.

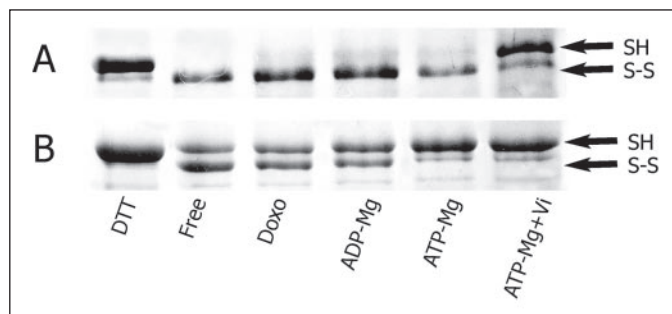


FIGURE 4. ATP/Mg binding triggers a conformational change moving the cysteine residue in the NBD away from the cysteine residue in the ICL1. After incubation at 25 °C for 30 min with either 5 mM DTT, 40 μM doxorubicin, 5 mM ADP, 5 mM ATP, or 0.5 mM Vi plus 5 mM ATP/Mg, the *E. coli* membrane vesicles containing the overexpressed S428C/T123C double mutant, with (*B*) or without (*A*) an additional E504Q mutation, were incubated with 200 μM CuSO_4 for 30 min at 30 °C and analyzed by SDS-PAGE without reducing agent.

functional cysteine-less BmrA mutant (24). The two residues mutated at the same time by a cysteine residue (Fig. 1, *B* and *C*) were separated by at most 9 Å in the open model (TABLE ONE). The double mutants thus created were S424C/N118C, S424C/A119C, S424C/T123C, M427C/V124C, M427C/V127C, S428C/T123C, S428C/V124C, and S428C/V127C. Interestingly, with the exception of M427C/V127C, all the double mutants predicted to be separated by less than 5 Å in the model, namely S424C/N118C, S424C/A119C, and S428C/V124C, were indeed able to form a disulfide bond in the presence of slightly oxidizing conditions. The fourth one, S428C/T123C, separated by 3.8 Å in the model, was even able to form a disulfide bond spontaneously without the addition of cupric ion as a catalyzer. By contrast, the three double mutants whose residues were predicted to be separated by more than 7 Å in the open BmrA model were totally unable to form a disulfide bond (TABLE ONE).

Incubation of the S428C/T123C double mutant in a buffer deprived of oxygen almost totally prevented the S–S bond formation, whereas incubation with increasing concentrations of cupric ion progressively transformed the reduced cysteine residues into a disulfide bond (Fig. 3*A*). A further addition of dithiothreitol fully restored the cysteine residues to the reduced form. The ability to create a disulfide bond in several double mutants indicates that the two cysteine residues must be separated by only a few Å in the three-dimensional structure of BmrA. This validates our BmrA model and, consequently, suggests that the template used to create our model, *i.e.* the conformation of the monomer of MsbA within the EcMsbA open dimer, is valid as well. Indeed, three additional BmrA models were built, one based solely on the closed structure of VcMsbA and two chimeric ones based on VcMsbA for the transmembrane domain and on the three-dimensional structure of either BtuD or MJ0796 for the two NBDs. These two latter models allow positioning of the two ATP-binding sites at the NBDs interface, a feature generally assumed to reflect a conformation competent for the transport (6, 31). According to each of these three closed models, a comparison of the distances between the two residues chosen to be replaced jointly by two cysteine residues clearly ruled out the possibility that disulfide bonds would have been formed in either additional model (Fig. 2, *B–D* and TABLE ONE). Furthermore, using a fourth BmrA model based on the latest MsbA closed structure released (StMsbA) also revealed that the distances between the two cysteine residues would be incompatible with S–S bond formations (Fig. 2*E* and TABLE ONE).

The formation of disulfide bonds had strong consequences on the functioning of the transporter. It abolished the Hoechst transport activity, whereas restoring the reduced forms of BmrA by a subsequent addi-

Conformational Changes in a Multidrug ABC Transporter

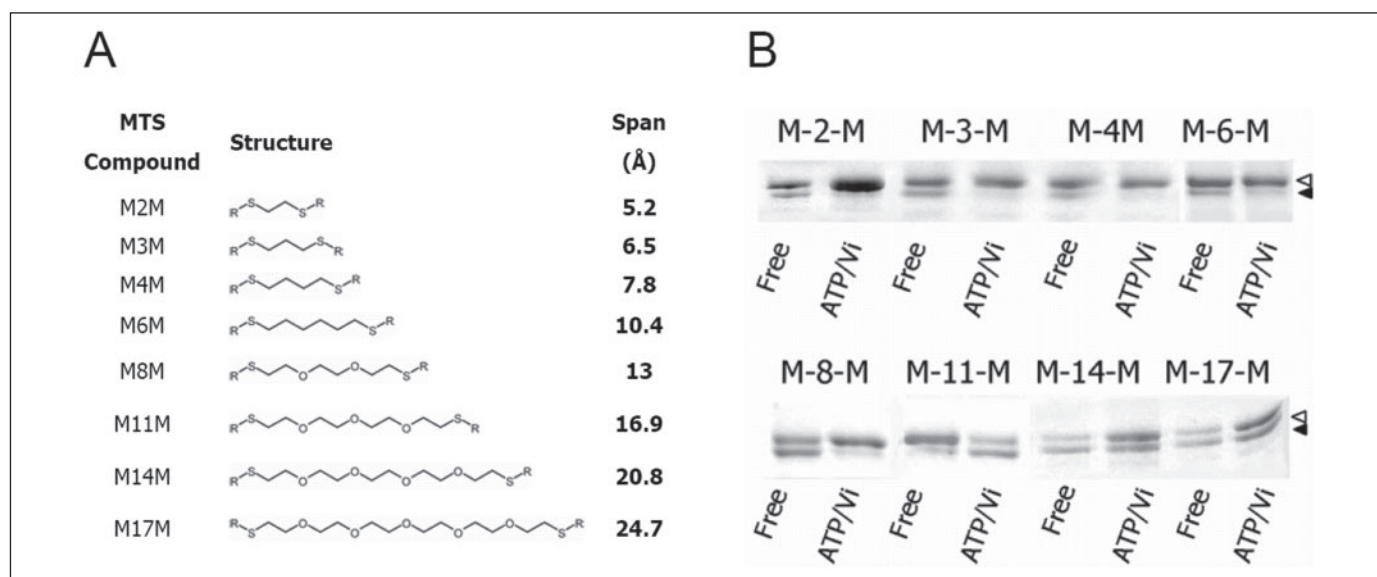


FIGURE 5. **The cross-linking of the two cysteine residues in the double mutant is still allowed, in the presence of ATP/Mg plus vanadate, by some homobifunctional reagents.** A, 200 μM methanethiosulfonate cross-linking reagent of different lengths was added to an ice-chilled suspension of *E. coli* membrane vesicles containing the overexpressed S428C/T123C double mutant either preincubated or not with 0.5 mM Vi plus 5 mM ATP/Mg at 25 °C for 30 min. B, free SH groups were derivatized by 10 mM *N*-ethylmaleimide, and samples were analyzed by SDS-PAGE without reducing agent. The white arrowhead indicates the position of BmrA with no intramolecular cross-link; the black arrowhead shows the position of BmrA containing an intramolecular cross-link. Panel A was adapted from Ref. 58.

tion of DTT allowed the recovery of its transport ability (Fig. 3B). In fact, formation of a disulfide bond drastically reduced the ATPase activity of BmrA (Fig. 3C). This bond formation most likely prevented a critical flexibility of the NBD, relative to ICL1, which seems to be mandatory to hydrolyze ATP. Indeed, chemical modification of cysteine residue(s) with *N*-ethyl-maleimide did not affect the ATPase activity of BmrA. It is important to note that prior chemical modification of BmrA prevented the disulfide bond formation catalyzed by a subsequent incubation with cupric ion, showing that at least one of the two cysteine residues of BmrA had been labeled by *N*-ethyl-maleimide.

The need for flexibility between the Q-loop and ICL1 for proper functioning of wild-type BmrA was further evidenced by the inhibitory effect afforded by ATP/Mg in the presence of vanadate on the S–S bond formation (Fig. 4). Moreover, a sharp decrease in S–S bond formation was observed in the presence of ATP/Mg alone, with the BmrA double mutant containing an additional E504Q mutation. This mutation has been shown to totally abolish ATP hydrolysis in BmrA and to induce a tight trapping of ATP/Mg, presumably at the NBDs interface (22).

To probe the relative displacement of the NBD from ICL1, homobifunctional cysteine-selective reagents of different lengths were used. Clearly, in the presence of ATP/Mg plus vanadate, an efficient intramolecular cross-linking between the two cysteine residues was mainly achieved when the length of the reagent was >13 Å (Fig. 5, solid triangle). It is important to note that the cross-linking reagents did not randomly cross-link cysteines between any two positions because no intramolecular bond formation could be achieved when the T123C/E504C double mutant was used as a negative control (not shown). However, because of the possible flexibility of these cross-linkers, it would be unreliable to quantify the distance separating the two cysteine residues in the vanadate-trapped conformation. However, it is reasonable to assume that a displacement of at least several Å of one domain relative to the other must have occurred to reach this vanadate-trapped conformational state.

DISCUSSION

A large body of evidence, including modification in tryptic digestion pattern (32, 33), quenching of the Trp intrinsic fluorescence (34), and

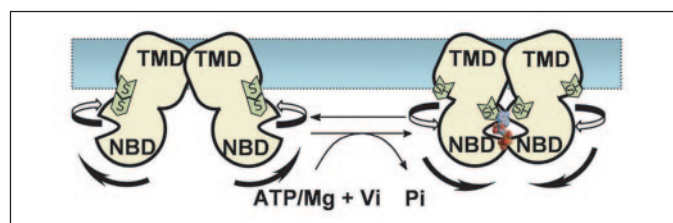


FIGURE 6. **Putative scheme to explain the disulfide bond formation, or prevention, in the BmrA double mutants.** This model is based on Chang's model (9), with one ATP molecule shown in color at the interface of the NBDs.

deuterium/hydrogen exchange profiles (35), has shown that global conformational changes are associated with the catalytic mechanism of ABC transporters. Accordingly, large domain movements have been detected in the low resolution three-dimensional structures of P-glycoprotein multidrug exporter (36, 37). On the other hand, based on three-dimensional structures of several NBDs either empty or loaded with different nucleotides (*i.e.* ATP or ADP), the Q-loop was proposed to be one of the most mobile elements of this domain (38, 39), and this was further supported by molecular dynamics studies of HisP (40, 41). Here, the physical displacement of the Q-loop of the NBD relative to ICL1 is directly demonstrated; furthermore, it is shown that this motion is mandatory for the proper functioning of wild-type BmrA. Indeed, ATP/Mg is thought to induce the dimerization of the two NBDs in a conformation where the two ATP-binding sites are shared between the NBDs (18, 19, 42), while addition of vanadate freezes the transporter in a subsequent transition state conformation (16). In the latter conformation, a reduction in the S–S bond formation was detected in the wild-type BmrA, indicating that the Q-loop has disengaged from ICL1. This result was exacerbated when the additional E504Q mutation was present in the double mutant; moreover, it was even observed in the absence of vanadate. This glutamate residue has been proposed to be the catalytic base of ABC transporters (18, 43, 44), and accordingly this mutation was shown to totally abolish ATP hydrolysis in BmrA (22). In fact, mutation of this Glu-504 in several residues, including the E504Q one, was also shown to induce a vanadate-insensitive tight trapping of ATP/Mg, most

likely at the NBDs interface of BmrA (22). This interpretation was consistent with the effects produced by equivalent mutations in other ABC transporters, *i.e.* a drastically altered ATP hydrolysis and a tight trapping of nucleotides (18, 42, 45–47). Therefore, it is reasonable to assume that ATP/Mg binding induces the dimerization of the two NBDs in BmrA, thereby moving the NBD away from ICL1 and thus preventing the disulfide bond formation. ICL1 would therefore act as a central pivot with the NBD moving around this TMD subdomain, conceivably by a hinge-like motion (48) that might involve as well a swiveling motion (9). In this way, the interaction between ICL1 and the Q-loop would be maintained throughout the catalytic cycle. This would be consistent with the three-dimensional structure of BtuCD, where the Q-loop is shown to mediate most of the NBD interactions with the TMD, and more precisely with the L-loop in this domain (also known as the “EAA” loop (49)) in a tightly packed conformation with the two ATP-binding sites located at the NBDs interface (8). The L-loop, which has been proposed to be functionally equivalent to ICL1 of MsbA (50) and to the N-terminal domain of the DrrB subunit of the daunorubicin/doxorubicin transporter (51), plays a key role in the function of ABC importers, and its interaction with the Q-loop is modulated by nucleotides (49, 52). This assumption also agrees, on the one hand, with the molecular dynamics studies of HisP and, on the other hand, with the conformations of the NBD loaded with different nucleotides (*i.e.* ATP or ADP), both showing that the Q-loop is one of the most mobile elements of this domain (38, 40).

As emphasized previously, one cannot accurately determine the displacement of the NBD from ICL1 induced by ATP-Mg binding (see Fig. 5). However, the stably trapped BmrA conformation thus generated either by the presence of vanadate or by the additional E504Q mutation is consistent with the two chimeric models based on either BtuD or MJ0796 three-dimensional structures, where the two ATP-binding sites are positioned at the NBDs interface (18). According to these two models and whatever the double mutants considered, the estimated distances between the two cysteine residues in an ATP/Mg bound conformation of BmrA would be at least 11.3 Å, a distance too long to allow a disulfide bond formation. On the other hand, according to the BmrA model solely based on the closed VcMsbA, no distances shorter than 18.4 Å would be expected between two cysteine residues. Recently, a new structure of MsbA was published that probably corresponds to a post-hydrolytic step (ADP + vanadate present in one of the NBDs) (10). Using this new structure as a template to model BmrA gave essentially the same results for the distances between the newly introduced cysteine residues as those presented in the table for the hybrid models: the shorter distance, 9.1 Å, was obtained for the double mutant S424C/N118C, whereas all other double mutants gave distances above 13.6 Å. Moreover, this new model also explains the prevention of disulfide bond formation observed for the double mutant in the presence of ATP/Mg plus vanadate (see Fig. 4; transition state akin to the new MsbA structure), whereas ATP/Mg alone was sufficient when an additional E504Q mutation was present (structure related to MJ0796 with two ATP/Mg sandwiched at the NBDs interface). Both BmrA models are indeed compatible with our overall conclusions that the two cysteine residues become too far apart to cross-link in either the pre-hydrolytic step (ATP binding) or the transition state (ADP trapped by vanadate).

A possible scheme to explain our results is depicted in Fig. 6. Although the findings reported here with BmrA only validate the conformation of monomeric EcMsbA and not necessarily the whole open dimer, we assume that in the resting state BmrA dimer is able to adopt an open conformation. In fact, a recent report using both intermolecular disulfide bonds and a spin labeling approach supports the existence

of an open MsbA dimer (53) and appears inconsistent with alternative models that have been proposed for a dimeric state of EcMsbA (12, 13). However, the open conformation in BmrA is likely to be energetically less favorable than a closed conformation akin to the BtuCD structure. Indeed, we have recently obtained evidence from fluorescence energy transfer experiments that, in the resting state, BmrA dimers preferentially adopt a closed conformation (24). Therefore, we propose that in the absence of nucleotides, BmrA dimers can explore different conformations between an open conformation akin to EcMsbA and a closed conformation akin to BtuCD (for the relative orientation of the NBDs), the latter conformation being found for most BmrA dimers at any given time. Formation of disulfide bonds will progressively displace the equilibrium toward the open dimer, whereas adding ATP/Mg plus vanadate to the wild-type transporter, or only ATP/Mg to the E504Q mutant, will maintain BmrA in a closed conformation, thereby lowering the likelihood of forming a disulfide bond between ICL1 and NBD. The great flexibility and possibly the rotation of NBDs relative to TMDs could be a peculiar feature of half-ABC transporters because both domains are only tethered through a long connecting loop that precedes the NBD. This loop appears quite flexible in MsbA (9), and it might act as a loose “leash” to maintain the NBD in close proximity to the TMDs without restraining its motion. Throughout the different conformations of the half-ABC transporter, contacts between NBDs and TMDs might be secured by ICL1 that would thus play a central role in interconnecting these two domains, as evidenced from either mutational (54–56) or structural studies (7, 9). By contrast, in full-length transporters such as Pgp, or even in ABC importers where the different domains are borne on separate polypeptides, the NBDs motion might be more restricted (57) and, for instance, swing back and forth in a tweezers-like motion (19) without any swiveling motion.

Acknowledgments—We thank Professor Frances J. Sharom for critical reading of the manuscript. We thank Dr. Geoffrey Chang for providing the atomic coordinates of MsbA before they were released.

REFERENCES

- Higgins, C. F. (1992) *Annu. Rev. Cell Biol.* **8**, 67–113
- Borst, P., and Elferink, R. O. (2002) *Annu. Rev. Biochem.* **71**, 537–592
- Haimeur, A., Conseil, G., Deeley, R. G., and Cole, S. P. (2004) *Curr. Drug Metab.* **5**, 21–53
- Van Bambeke, F., Balzi, E., and Tulkens, P. M. (2000) *Biochem. Pharmacol.* **60**, 457–470
- Holland, I. B., and Blight, M. A. (1999) *J. Mol. Biol.* **293**, 381–399
- Davidson, A. L., and Chen, J. (2004) *Annu. Rev. Biochem.* **73**, 241–268
- Chang, G., and Roth, C. B. (2001) *Science* **293**, 1793–1800
- Locher, K. P., Lee, A. T., and Rees, D. C. (2002) *Science* **296**, 1091–1098
- Chang, G. (2003) *J. Mol. Biol.* **330**, 419–430
- Reyes, C. L., and Chang, G. (2005) *Science* **308**, 1028–1031
- Jones, P. M., and George, A. M. (2004) *Cell Mol. Life Sci.* **61**, 682–699
- Campbell, J. D., Biggin, P. C., Baaden, M., and Sansom, M. S. (2003) *Biochemistry* **42**, 3666–3673
- Shilling, R. A., Balakrishnan, L., Shahi, S., Venter, H., and van Veen, H. W. (2003) *Int. J. Antimicrob. Agents* **22**, 200–204
- Stenham, D. R., Campbell, J. D., Sansom, M. S., Higgins, C. F., Kerr, I. D., and Linton, K. J. (2003) *FASEB J.* **17**, 2287–2289
- Hopfner, K. P., Karcher, A., Shin, D. S., Craig, L., Arthur, L. M., Carney, J. P., and Tainer, J. A. (2000) *Cell* **101**, 789–800
- Fetsch, E. E., and Davidson, A. L. (2002) *Proc. Natl. Acad. Sci. U. S. A.* **99**, 9685–9690
- Loo, T. W., Bartlett, M. C., and Clarke, D. M. (2002) *J. Biol. Chem.* **277**, 41303–41306
- Smith, P. C., Karpowich, N., Millen, L., Moody, J. E., Rosen, J., Thomas, P. J., and Hunt, J. F. (2002) *Mol. Cell* **10**, 139–149
- Chen, J., Lu, G., Lin, J., Davidson, A. L., and Quijcho, F. A. (2003) *Mol. Cell* **12**, 651–661
- Steinfeld, E., Orelle, C., Fantino, J. R., Dalmas, O., Rigaud, J. L., Denizot, F., Di Pietro, A., and Jault, J. M. (2004) *Biochemistry* **43**, 7491–7502
- Reuter, G., Janvilisri, T., Venter, H., Shahi, S., Balakrishnan, L., and van Veen, H. W.

Conformational Changes in a Multidrug ABC Transporter

- (2003) *J. Biol. Chem.* **278**, 35193–35198
22. Orelle, C., Dalmas, O., Gros, P., Di Pietro, A., and Jault, J. M. (2003) *J. Biol. Chem.* **278**, 47002–47008
23. Steinfels, E., Orelle, C., Dalmas, O., Penin, F., Miroux, B., Di Pietro, A., and Jault, J. M. (2002) *Biochim. Biophys. Acta* **1565**, 1–5
24. Dalmas, O., Do Cao, M. A., Lugo, M. R., Sharom, F. J., Di Pietro, A., and Jault, J. M. (2005) *Biochemistry* **44**, 4312–4321
25. Combet, C., Jambon, M., Deleage, G., and Geourjon, C. (2002) *Bioinformatics* **18**, 213–214
26. Brunger, A. T., Adams, P. D., Clore, G. M., DeLano, W. L., Gros, P., Grosse-Kunstleve, R. W., Jiang, J. S., Kuszewski, J., Nilges, M., Pannu, N. S., Read, R. J., Rice, L. M., Simonson, T., and Warren, G. L. (1998) *Acta Crystallogr. Sect. D Biol. Crystallogr.* **54**, Pt. 5, 905–921
27. Geourjon, C., and Deleage, G. (1995) *J. Mol. Graph. Model.* **13**, 209–212, 199–200
28. Laskowski, R. A., MacArthur, M. W., Moss, D. S., and Thornton, J. M. (1993) *J. Appl. Crystallogr.* **26**, 283–291
29. Sali, A., and Blundell, T. L. (1993) *J. Mol. Biol.* **234**, 779–815
30. Brooks, B. R., Brucoleri, R. E., Olafson, B. D., States, D. J., Swaminathan, S., and Karplus, M. (1983) *J. Comput. Chem.* **4**, 187–217
31. Higgins, C. F., and Linton, K. J. (2004) *Nat. Struct. Mol. Biol.* **11**, 918–926
32. Wang, G., Pincheira, R., Zhang, M., and Zhang, J. T. (1997) *Biochem. J.* **328**, Pt. 3, 897–904
33. Julien, M., and Gros, P. (2000) *Biochemistry* **39**, 4559–4568
34. Sonveaux, N., Viganò, C., Shapiro, A. B., Ling, V., and Ruyschaert, J. M. (1999) *J. Biol. Chem.* **274**, 17649–17654
35. Sonveaux, N., Shapiro, A. B., Goormaghtigh, E., Ling, V., and Ruyschaert, J. M. (1996) *J. Biol. Chem.* **271**, 24617–24624
36. Rosenberg, M. F., Velarde, G., Ford, R. C., Martin, C., Berridge, G., Kerr, I. D., Callaghan, R., Schmidlin, A., Wooding, C., Linton, K. J., and Higgins, C. F. (2001) *EMBO J.* **20**, 5615–5625
37. Rosenberg, M. F., Callaghan, R., Modok, S., Higgins, C. F., and Ford, R. C. (2005) *J. Biol. Chem.* **280**, 2857–2862
38. Yuan, Y. R., Blecker, S., Martsinkevich, O., Millen, L., Thomas, P. J., and Hunt, J. F. (2001) *J. Biol. Chem.* **276**, 32313–32321
39. Verdon, G., Albers, S. V., Dijkstra, B. W., Driessen, A. J., and Thunnissen, A. M. (2003) *J. Mol. Biol.* **330**, 343–358
40. Jones, P. M., and George, A. M. (2002) *Proc. Natl. Acad. Sci. U. S. A.* **99**, 12639–12644
41. Campbell, J. D., Deol, S. S., Ashcroft, F. M., Kerr, I. D., and Sansom, M. S. (2004) *Biophys. J.* **87**, 3703–3715
42. Moody, J. E., Millen, L., Binns, D., Hunt, J. F., and Thomas, P. J. (2002) *J. Biol. Chem.* **277**, 21111–21114
43. Muneyuki, E., Noji, H., Amano, T., Maseike, T., and Yoshida, M. (2000) *Biochim. Biophys. Acta* **1458**, 467–481
44. Geourjon, C., Orelle, C., Steinfels, E., Blanchet, C., Deleage, G., Di Pietro, A., and Jault, J. M. (2001) *Trends Biochem. Sci.* **26**, 539–544
45. Janas, E., Hofacker, M., Chen, M., Gompf, S., van der Does, C., and Tampe, R. (2003) *J. Biol. Chem.* **278**, 26862–26869
46. Payen, L. F., Gao, M., Westlake, C. J., Cole, S. P., and Deeley, R. G. (2003) *J. Biol. Chem.* **278**, 38537–38547
47. Tomblin, G., Bartholomew, L. A., Urbatsch, I. L., and Senior, A. E. (2004) *J. Biol. Chem.* **279**, 31212–31220
48. Gerstein, M., Lesk, A. M., and Chothia, C. (1994) *Biochemistry* **33**, 6739–6749
49. Mourez, M., Hofnung, M., and Dassa, E. (1997) *EMBO J.* **16**, 3066–3077
50. Locher, K. P. (2004) *Curr. Opin. Struct. Biol.* **14**, 426–431
51. Kaur, P., Rao, D. K., and Gandlur, S. M. (2005) *Biochemistry* **44**, 2661–2670
52. Hunke, S., Mourez, M., Jehanno, M., Dassa, E., and Schneider, E. (2000) *J. Biol. Chem.* **275**, 15526–15534
53. Buchaklian, A. H., Funk, A. L., and Klug, C. S. (2004) *Biochemistry* **43**, 8600–8606
54. Currier, S. J., Kane, S. E., Willingham, M. C., Cardarelli, C. O., Pastan, I., and Gottesman, M. M. (1992) *J. Biol. Chem.* **267**, 25153–25159
55. Kwan, T., and Gros, P. (1998) *Biochemistry* **37**, 3337–3350
56. Ambudkar, S. V., Dey, S., Hrycyna, C. A., Ramachandra, M., Pastan, I., and Gottesman, M. M. (1999) *Annu. Rev. Pharmacol. Toxicol.* **39**, 361–398
57. Qu, Q., and Sharom, F. J. (2001) *Biochemistry* **40**, 1413–1422
58. Loo, T. W., and Clarke, D. M. (2001) *J. Biol. Chem.* **276**, 36877–36880

The Q-loop Disengages from the First Intracellular Loop during the Catalytic Cycle of the Multidrug ABC Transporter BmrA
Olivier Dalmas, Cédric Orelle, Anne-Emmanuelle Foucher, Christophe Geourjon, Serge Crouzy, Attilio Di Pietro and Jean-Michel Jault

J. Biol. Chem. 2005, 280:36857-36864.

doi: 10.1074/jbc.M503266200 originally published online August 17, 2005

Access the most updated version of this article at doi: [10.1074/jbc.M503266200](https://doi.org/10.1074/jbc.M503266200)

Alerts:

- [When this article is cited](#)
- [When a correction for this article is posted](#)

[Click here](#) to choose from all of JBC's e-mail alerts

This article cites 58 references, 22 of which can be accessed free at <http://www.jbc.org/content/280/44/36857.full.html#ref-list-1>